http://dx.doi.org/10.5012/bkcs.2013.34.6.1715

Magnetization of Magnetite Ferrofluid Studied by Using a Magnetic Balance

Daeseong Jin and Hackjin Kim*

*Department of Chemistry, Chungnam National University, Taejeon 305-764, Korea. *E-mail: hackjin@cnu.ac.kr*
Received February 7, 2013, Accepted March 15, 2013

Magnetic properties of magnetite ferrofluid are studied by measuring magnetic weights under different magnetic fields with a conventional electronic balance. Magnetite nanoparticles of 11 nm diameter are synthesized to make the ferrofluid. Magnetization calculated from the magnetic weight reveals the hysteresis and deviates from the Langevin function at high magnetic fields. Magnetic weight shifts instantaneously with magnetic field change by Neel and Brown mechanism. When high magnetic field is applied to the sample, slower change of magnetic weight is accompanied with the instantaneous shift *via* agglomeration of nanoparticles. The slow change of the magnetic weight shows the stretched exponential kinetics. The temporal change of the magnetic weight and the magnetization of the ferrofluid at high magnetic fields suggest that the superparamagnetic sample turns into superspin glass by strong magnetic interparticle interactions.

Key Words : Magnetite, Ferrofluid, Superparamagnetic, Stretched exponential, Magnetic interactions

Introduction

Magnetic nanoparticles have attracted many researchers for their wide applications in various fields.[1-6] Efficient synthetic methods of well-characterized magnetic nanoparticles have been developed, and theranostic applications such as hyperthermia, drug delivery and MRI contrast enhancement have been important interdisciplinary research topics these days. Magnetite, ferrimagnetic iron oxide Fe_3O_4 which is one of the most magnetic minerals naturally occurring, has been used as magnetic recording medium and ferrofluid in electronic and mechanical engineering. Magnetite nanoparticles with modified surface[7] or combined with biomolecules[8] show unique characteristics. Nanocomposite magnetite particles formed by self-assembly play multifunctional roles in different environments.[9,10] While magnetite nanoparticles are one of the most studied nanomaterials, many of their interesting magnetic behaviors in various conditions remain to be investigated.

Nanosize ferro- or ferrimagnetic particles with sufficient thermal energy move continuously in low concentration ferrofluids so that magnetic moments are randomly oriented in space to give zero remanent magnetization, which is called superparamagnetic. Superparamagnetic nanoparticles show relaxation of magnetization following Neel and Brown mechanism.[11] When interparticle interactions are negligible in the ferrofluids, the magnetization process obeys the Arrhenius type kinetics. Magnetite nanoparticles reveal different magnetic properties that greatly depend on the concentration,[12] the solvent,[13] the particle size distribution,[14] the preparation method of particles,[15] so on. When thermal energy of nanoparticles reduces at low temperatures[11] or interparticle dipolar interactions become significant at high concentrations[16] or nanoparticles are fabricated by various methods,[17-19] superparamagnetic properties of ferrofluid alter prominently. Changes of interparticle interactions induce phase transitions of magnetic nanoparticle samples from superparamagnetic to paramagnetic, superspin glass or superferromagnetic, and a simple relaxation dynamics turns into complicated ones.[20-22] Magnetic field enhances interparticle interactions in magnetic nanomaterials to provoke many chemical, rheological and topological changes. Under magnetic field, highly crystalline magnetite particles have been synthesized[23] and aggregates of nanoparticles for sensitive spectroscopic detection have been prepared.[24] By applying magnetic field to ferrofluids, nanoparticles of fluids can be displaced, isolated and agglomerated to show famous spike patterns. Various photographic images have been reported to elucidate the involved dynamics of magnetic nanoparticles.[25-28]

In this work, the magnetization of magnetite nanoparticles is studied by measuring the magnetic weight change of magnetite ferrofluid with a conventional electronic balance. When magnetic field is applied to the ferrofluid, magnetic weight of the sample shifts instantaneously by Neel and Brown relaxation. Magnetic nanoparticles agglomerate to form a dense ferrofluid above a threshold magnetic field. Agglomeration is a kind of self-organization occurring over various energy barriers that evolve during the dynamic changes. Morphological changes and hysteresis of magnetization by strong interparticle interactions are observed above the threshold field. Slow structural relaxation by interparticle interactions reveals non-exponential time dependence. Temporal and morphological changes of ferrofluid at high magnetic field suggest that the superparamagnetic ferrofluid experiences phase transitions involving collective states of nanoparticles.

Experimental

Many reliable preparation methods of well-defined magnetite nanoparticles have been reported.[29-32] In this work, round shape magnetite nanoparticles with narrow size distri-

bution are synthesized by reacting iron(II) and iron(III) chloride salts in aqueous ammonia solution. Tetramethylammonium hydroxide is used as a surfactant to stabilize the magnetite nanoparticles in aqueous solution. The synthesized magnetite nanoparticles have been stable at room temperature for several months. The XRD pattern of the synthesized nanoparticles confirms the well-known magnetite phase of high purity[32] and the TEM images show that the nanoparticles have the diameter of 11 nm with narrow distribution. The TEM images and the XRD pattern are given in the Supporting Information. The magnetite concentration of the ferrofluid studied in this work is 3 wt % or less.

Figure 1 shows the experimental setup for the measurement of magnetic weight of ferrofluid. While the magnetic field is perpendicular to the gravity in the Gouy balance, the magnetic force in this work is parallel to the gravitational force as in the Rankine balance[33] which is the more sensitive. The force exerted by magnetization of the sample contained in a vial is directly measured with a conventional electronic balance [Denver Inst. SI-234 230 g × 0.1 mg]. The magnetic field is varied by moving the NdFeB disc magnet on the precision translation stage. The magnet does not affect the balance much. When the magnet is close to the balance to apply low magnetic fields to the sample, high fields are applied to the balance and the balance changes by less than 10 mg, which is tolerable in this work. As the magnet is moved to the sample to apply high fields, the magnetic weight increases up to a few grams at high fields and the effect of magnet field on the balance is less than 1 mg. Especially when the magnet is located close to the sample for the study of temporal changes at high magnetic fields, the magnet is far distant from the balance, which does not affect the balance at all. Figure 1(b) shows the magnetic field strength measured with a magnetometer [Kanetec teslameter TM-701] at different positions between the sample and the magnet. Since the vertical component of the magnetic force, F_z is attributed to the magnetic weight Δm of the sample with volume V_{sample}, the magnetic force measured with the balance is given by

$$F_z = (\Delta m)g = [V_{sample}\, M\, (\nabla \mathbf{B})]_z \quad (1)$$

where g is the acceleration of gravity, M is the magnetization of the sample and $\nabla \mathbf{B}$ is the gradient of the inhomogeneous field from the magnet. Inset of Figure 1(b) shows the magnetic field gradient evaluated with the measured magnetic field. The magnetic field gradient in this work is regarded as low gradient range, < 100 T/m in the magnetic separation.[28]

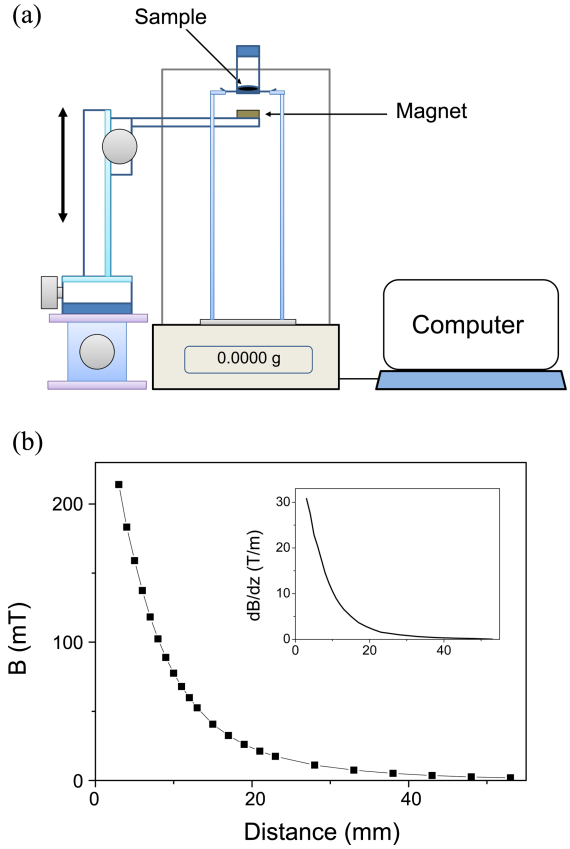

Figure 1. (a) Magnetic weight by magnetization of the sample is measured with an electronic balance connected to a computer. (b) Magnetic field strength measured at different positions between the sample and the magnet. Inset shows the magnetic field gradient evaluated from the measured magnetic field.

Results and Discussion

Magnetization from Magnetic Weight Measurement. Figure 2(a) shows the magnetic weights of the 1 mL ferrofluid sample containing 3 wt % magnetite nanoparticles at different magnetic fields. The ferrofluid is ~2 mm thick. The magnetite nanoparticles keep dispersed well in the solution during the measurement of magnetic weights. Under low magnetic fields, the magnetic weight shifts instantaneously with the field change and does not alter afterwards. However, the magnetic weight varies slowly after an instantaneous shift when the applied magnetic field is higher than ca. 35 mT. The magnetic weights of Figure 2(a) are measured at 5 min after the magnetic field is set. In order to measure the steady-state magnetic weight above the threshold magnetic field, we should wait more than 2 days. Temporal changes of the magnetic weight are discussed in section B. Hysteresis of the magnetic weight and evident morphological changes of the ferrofluid sample begin to arise above the threshold field. The morphological changes of the sample are discussed in detail in section C. A greater hysteresis of magnetic weight is observed when the holding time at a given magnetic field is longer. The threshold magnetic field is lower for the sample with higher magnetite concentration.

The magnetizations of the sample at different magnetic fields of Figure 2(b) are calculated with Eq. (1) and the magnetic weights. Superparamagnetism of the magnetite sample is confirmed from the zero remanent magnetization. Hysteresis of the magnetization is clearly observed. The zero remanent magnetization and the hysteresis of the magnetization indicate that the sample is superparamagnetic at low magnetic fields but not above the threshold magnetic field. Magnetic phase transitions occur by temperature and pressure change

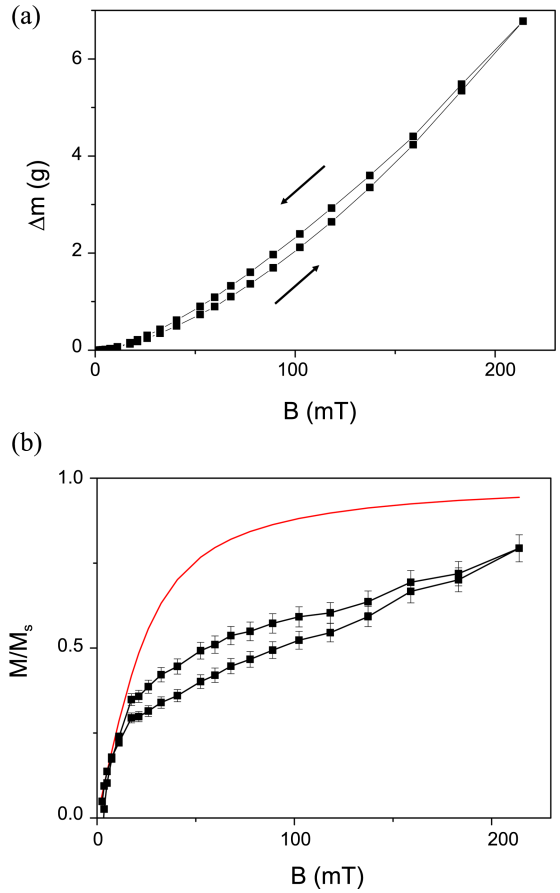

Figure 2. (a) Magnetic weight of the 3 wt % sample at different magnetic fields. As the magnetic weight changes slowly following an instantaneous shift at high fields, it is measured at 5 min after the magnetic field is set. (b) Magnetization of the sample calculated from Eq. (1), the magnetic weights of Figure 2(a) and the magnetic field gradient of Figure 1(b). The curve above the magnetization data represents the Langevin function.

as well as substantial changes of interparticle interactions that result from clustering, concentration increase or magnetic field application.[34]

In Figure 2(b), the magnetization of the sample is normalized with the saturation magnetization of 4.1×10^5 A/m which is ~90% of the bulk saturation magnetization of magnetite, $M_{sat} \approx 4.7 \times 10^5$ A/m[28]. The curve above the measured magnetization represents the Langevin function, $L(x) = \coth(x) - 1/x$ where x is given by the ratio of magnetic and thermal energy.[11,35] With this saturation magnetization value, the magnetization data and the Langevin curve come close at high magnetic field. The saturation magnetization of magnetic nanoparticles is usually smaller than the saturation magnetization of bulk sample because of surface disorders and other anisotropies of nanoparticles. For magnetite nanoparticles, the saturation magnetizations of 70% to 100% of the bulk saturation magnetization have been reported.[7,36,37] The relatively large saturation magnetization of the sample is rather considered to result from magnetic phase transition of the sample at high magnetic fields that is discussed below.

The Langevin function is a good approximation for the magnetization at high temperatures where the anisotropy energy of superparamagnetic nanoparticles is smaller than thermal energy. If the bulk saturation magnetization is employed for the data of Figure 2(b), the Langevin curve goes up slightly without appreciable change of overall curve shape so that the difference between the curve and the measured magnetization becomes larger. Phase transition that modifies the magnetic properties of the sample significantly is considered to result in the mismatch between the Langevin curve and the measured magnetization, and the different slopes of the two magnetization data above the threshold magnetic field. The Langevin curve becomes close to saturation above 100 mT, but the measured magnetization seems to be in the middle of change even above 200 mT. These difference of magnetization suggest that the ferrofluid sample above the threshold is not superparamagnetic.

Smaller magnetization than the estimation with the Langevin function is due to the decease of the susceptibility at high magnetic fields. The initial magnetic susceptibility evaluated from the slope of the measured magnetization at low fields where the magnetization grows linearly with the magnetic field, is 2×10^6 in the SI unit, which is in the range of reported values for magnetite nanoparticles of similar sizes, 1×10^6 to 5×10^6.[38] The magnetization of a spin glass is expressed as a power series in the magnetic field, H as[11,39]

$$M = \chi_1 H - \chi_3 H^3 + \chi_5 H^5 - \cdots \quad (2)$$

where χ's are the magnetic susceptibilities. Considering that the nonlinear susceptibility χ_3 diverges near the phase transition to superspin glass, difference of the two magnetization data above the threshold can be understood as a result of the phase transition to superspin glass. As the magnetic weight changes steadily during the measurement, the χ_3 cannot be determined exactly from the data of Figure 2(b), however, the order of magnitude of the roughly estimated χ_3 can give a clue to the validity of the phase transition of the sample. When only first two terms of Eq. (2) are considered for the magnetization above the threshold, the χ_3 is estimated to be in the range of 7×10^{-5} to 1×10^{-3} m^2/A^2. Only a few cases have been reported for the χ_3 values of nanomaterials near phase transition and the χ_3 of ferromagnetic single domain CoFe nanomaterials is reported to be in the order of 10^{-3} m^2/A^2 around the phase transition.[40] Although the χ_3 value varies greatly for different materials, the χ_3 estimated above for the magnetite nanoparticle seems to lie in the reasonable range, which supports that the phase transition of superparamagnetic sample to superspin glass occurs above the threshold magnetic field.

Temporal Changes of Magnetic Weight. Figure 3 shows a temporal change of the magnetic weight of the 3 wt % sample after it is placed at the magnetic field of 212 mT. The magnetic weight was read every minute. At t = 0, the magnetic weight already made the instantaneous shift *via* Neel and Brown mechanism of magnetization. The two mechanisms work in the time scale much shorter than a second at room temperature.[14] Since the response time of the electronic balance used in this work is 2 sec, the effect of mag-

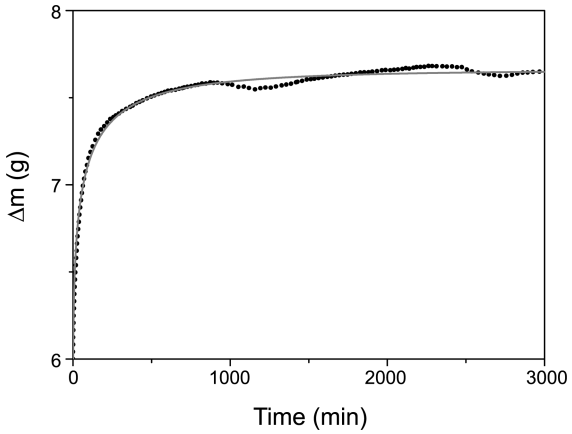

Figure 3. Temporal change of magnetic weight of the 3 wt % sample when the sample is placed at magnetic field of 212 mT. Fitting curve of the stretched exponential function of Eq. (3) is overlapped and the analysis results are given in Table 1.

netization by the two mechanisms appears instantaneously in the magnetic weight. The instantaneous shift of the magnetic weight under the magnetic field is a few % smaller than the value reached by the stepwise application of the field in Figure 2(a). The slow change of the magnetic weight above the threshold magnetic field is attributed to mechanisms other than Neel and Brown mechanism.

After the instantaneous shift, the magnetic weight seems to increase to a maximum around 1000 min and then grows more slowly with fluctuating. The fluctuation of the magnetic weight is ascribed to the daily variation of laboratory temperature. The maximum around 1000 min is not the true one. The temperature effect is clearly observed when the change of the magnetic weight is small compared with thermal energy variance as like after ~1000 min. Most of nanoparticles of the sample agglomerate within an hour, long before the maximum is observed. Main growth of the magnetic weight takes place during the contraction of the agglomerate. The temporal change of the magnetic weight fits well with the stretched exponential function called the Kohlrausch-Williams-Watts (KWW) function,[41,42]

$$m(t) = m(\infty) + [m(0) - m(\infty)] \exp[-(t/\tau)^{\beta}] \quad (3)$$

where τ is the effective relaxation time constant and β is a parameter inversely related to the width of the involved energy barrier distribution. Since $0 < \beta < 1$, the function is called the stretched exponential. Average relaxation time of the stretched exponential dynamics is given by $\langle\tau\rangle = (\tau/\beta)\,\Gamma(1/\beta)$ where Γ is the gamma function. The parameters given in Table 1 are determined from the analysis of temporal change data up to ~1000 min before the effect of thermal energy fluctuation appears. The temporal change of the magnetic weight is highly reproducible. Slower development of magnetization than Neel and Brown mechanism indicates that the sample is not superparamagnetic but in the collective states where interparticle interactions are evident.

The stretched exponential relaxation (SER) is a dominant character of disordered or self-organized systems.[43] For the dynamics of magnetic nanomaterials, several non-exponential relaxation kinetics including the SER have been reported.[11,21,22] Decay of magnetization of superspin glass follows the SER at low concentration and turns into a power law like t^{-n} with the increase of concentration. This behavior results from the interparticle interactions which increase with the concentration. Superferromagnetic domains with the non-zero remanent magnetization appear when the interparticle interactions become large enough to make a long range ordered state beyond the superspin glass. Superferromagnetism is attributed to high concentration and percolation of nanoparticles.

Agglomeration of nanoparticles by interparticle interactions accounts for the slow increase of the magnetic weight described with the SER which confirms the formation of superspin glass. Agglomeration is a kind of structural relaxation occurring by magnetic field gradient in the direction of gravity in this work. The magnetic weight increases still even after most nanoparticles agglomerate, which indicates that the structural relaxation looking for the lowest energy configuration undergoes inside the agglomerate. For the SER in glass, a diffusion-trap model predicts that $\beta = 3/5$ for stress relaxation and $\beta = 3/7$ for thermal structural relaxation.[44] As nanoparticles agglomerate under the unidirectional magnetic field, the dimension of the agglomeration is restricted in this work. Because two processes with different characters, agglomeration and then structural relaxation inside the agglomerate occur in the dynamics, it is not easy to deduce a single value for the stretching exponent. If the slower growth of the magnetic weight after ~1000 min is included in the data fitting, the stretching exponent decreases and the effective relaxation time as well as the average relaxation time increases. Since the magnetic weight increases steadily even after ~1000 min, extending the fitting range naturally makes the relaxation times longer. Slower growth of the magnetic weight corresponds to higher energy barriers. Adding processes with higher energy barriers to a dynamics makes the involved energy barrier spectrum broaden, which reduces the stretching exponent that is inversely proportional to the width of the energy barrier distribution.

Larger stretching exponent at lower magnetic field implies that the energy barrier spectrum is narrower at lower field and the relaxation dynamics is simpler at lower field. How-

Table 1. The kinetic parameters for magnetic weight change of 3 wt % sample with Eq. (3)

m(0)(g)[a]	[m(∞) – m(0)](g)	β	τ (min)	<τ> (min)[b]
6.070 ± 0.137	1.714 ± 0.012	0.548 ± 0.023	56.6 ± 4.1	53.2 ± 4.5

[a]Instantaneous magnetic weight shift by Neel and Brown mechanism. [b]The average relaxation time.

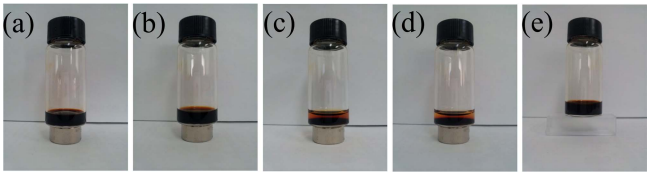

Figure 4. Temporal change of the 3 wt % sample morphology under magnetic field of 228 mT. (a) Just after the sample vial is placed on the magnet, the ferrofluid forms a swollen dome. (b) After 2 h on the magnet, the swollen ferrofluid contracts by agglomeration of nanoparticles and this makes the convex meniscus of the ferrofluid solution concave. The opaque solution turns into brown solution with black agglomerate at the bottom. (c) After 24 h on the magnet, the agglomerate shrinks to *ca.* 1 mm thick and the color of solution becomes thinner. (d) After 48 h on the magnet, the agglomerate looks unchanged and the color of the solution almost disappears as the nanoparticles of the solution join the agglomerate. (e) As soon as the magnet is removed, the ferrofluid returns to the original opaque solution before applying the magnetic field.

ever, the relaxation time is observed to be much longer at lower field. If the relaxation of the magnetic weight is a process where the perturbation by magnetic field decays, the relaxation time would be shorter at lower field. Longer relaxation time at lower field indicates that the relaxation is driven by magnetic force. Magnetic field builds up interparticle interactions and works as a driving force for the relaxation under magnetic field.

Morphological Changes of Ferrofluid under Magnetic Field. When ferrofluids containing a few tens wt % of magnetite are exposed to magnetic field, well-known spike patterns of asperities are produced.[26] The spike patterns are observed when the ferrofluid concentration is high. The samples used in this work are the aqueous solutions containing 3 wt % or less magnetite, therefore, the spike patterns form only when magnetite nanoparticles are decanted with a magnet after synthesis. Figure 4 shows photographic images of morphological changes of the 3 wt % ferrofluid when it is placed at the magnetic field of 228 mT. Dark brown ferrofluid swells up instantaneously when the applied magnetic field is greater than the threshold. As the swollen ferrofluid contracts slowly by agglomeration of nanoparticles, the opaque solution turns into a transparent solution with black agglomerate at the bottom. The convex meniscus of the swollen ferrofluid becomes concave when dense agglomerate forms after several hours. If all the nanoparticles percolate into the agglomerate as in the crystalline magnetite, the thickness of the agglomerate would be *ca*. 20 mm. The agglomerate is not so thin in the solution because thermal energy of nanoparticles hinders close packing. After more than 48 h, the dark ferrofluid turns into a totally clear solution with magnetite at the bottom. The agglomerate formed by staying under magnetic field longer than 48 h keeps its shape if the magnetic field is removed very gently, however, it is readily redispersed by a small perturbation.

Agglomeration, morphological change of ferrofluid by magnetic field is a kind of externally directed self-assembly. At the beginning of the dynamics where the energy barrier is low, distant particles agglomerate *via* field-induced interparticle interactions and local flows. Before the magnetic weight reaches the maximum around 1000 min, the energy barrier rises with the increase of interparticle interactions, which make the agglomerate contract gradually. Around 1000 min, the agglomerate becomes quite stable but its configuration is not at the energy minimum yet. Even afterwards nanoparticles migrate slowly but constantly inside the agglomerate, that is, the structural relaxation of the agglomerate persists but the energy barrier is too high to find the energy minimum swiftly. It takes a long time the agglomerate to make the configuration of the lowest energy, which would appear as the true maximum of magnetic weight. During the dynamic change, interparticle interactions increase drastically as reflected in the stretched exponential kinetics. Agglomeration itself is an evidence of the phase transition of the superparamagnetic sample. The agglomerate that keeps its shape after removing the magnetic field represents a long range ordered state and the non-zero remanent magnetization. The metastable agglomerate indicates that the superferromagnetic state is formed at the end of agglomeration.

Time for Agglomeration. It takes an hour the swollen ferrofluid under magnetic field to turn into light brown solution with black agglomerate as shown in Figure 4. The magnetophoretic velocity v for estimating the agglomeration time can be deduced by balancing the magnetic force of Eq. (1) and the viscous drag $F_d = 6\pi R\eta v$ where R is the radius of the particle and η is the viscosity of the solvent.[45] Here, no interparticle interactions are assumed. In our case, the magnetophoretic velocity is 7.8×10^{-8} m/sec. It takes 7 hours the agglomerate to form after the nanoparticles travel the distance of the sample thickness. Interparticle interactions make the agglomeration time shorter than expected from the magnetophoretic velocity, however, our agglomeration time of an hour is much longer than usually observed in the separation experiments using the magnet field of similar gradient.[25,28,45] In the separation experiment, it takes only a few minutes the solution to become clear.

Magnetophoretic separation time has been evaluated with a simple empirical model that compares thermal energy and magnetic dipolar energy at low gradient magnetic field.[45] In the model, the nanoparticles separate by magnetic dipolar interactions and the separation time t_s required for the opacity of the solution to decay to 10% of the initial value is given by

$$t_s = t_o [d/\lambda_B]^{\alpha} \quad (4)$$

where the time constant t_o and the exponent a are the empirically determined constants, d is the interparticle distance that can be estimated from the concentration, and λ_B is the magnetic Bjerrum length that can be calculated with magnetization, particle size, and temperature. The Bjerrum length is the distance between magnetic dipole particles where magnetic interaction energy is comparable with thermal energy. When the Bjerrum length is greater than the particle diameter, the nanoparticles aggregate. We have all the parameters to calculate the separation time for our case if the

empirically determined parameters, t_o and α of Ref. 45 are employed; d = 49 nm, λ_B = 15 nm and t_s = 156 sec. Large difference between the observed and the estimated separation time is mainly attributed to the different experimental setups for applying magnetic field. A disc magnet is used in our experiments and a ring type magnet surrounding a sample is used in many magnetic separation setups. It should be noticed that the empirically determined constants of Eq. (4) have the values unique to the experimental conditions and the sample concentration. In the ring type separation setup, the separation time shows a weak concentration dependence, $t_s \propto c^{-0.24}$, which tells that the concentration change by ~20 times makes the separation time twice. In our experiments, only a small change of concentration or sample amount affects the separation time significantly. When the swelling of the ferrofluid sample reduces by dilution, the agglomeration time increases conspicuously. The morphological change of swelling that deeply depends on interparticle interactions is more critical for the agglomeration of nanoparticles than the magnetophoretic velocity in solution.

Concluding Remarks

Magnetite nanoparticles in a dilute solution as in this work, are superparamagnetic at room temperature.[6-8] The zero remanent magnetization of the sample and the complete redispersion after the cyclic application of the magnetic field confirm that the sample is superparamagnetic. Magnetic properties of dilute nanoparticle solutions vary by alteration of interparticle interactions, that is, mainly magnetic dipolar interactions. The magnetic phase transition results from competition between magnetic and thermal energy of magnetic nanoparticles. Superparamagnetic solution may turn into superspin glass or superferromagnetic without temperature change if interparticle interactions increase greatly. As the magnetic dipolar interaction is inversely proportional to the interparticle distance ($\propto r^{-3}$), the concentration change can modify magnetic properties of ferrofluids.

Interparticle interactions of the magnetite nanoparticles at high magnetic fields result in the morphological change of swelling and agglomeration, the hysteresis of magnetization observed by the magnetic weight, and the mismatch between the magnetization and the Langevin curve. These observations indicate that the sample is not superparamagnetic above the threshold magnetic field. The roughly estimated nonlinear susceptibility and the stretched exponential kinetics of magnetization confirm that the agglomerate of the ferrofluid sample is superspin glass above the threshold. The agglomerate annealed under the magnetic field keeps its shape after removal of the magnetic field, which suggests that the annealed agglomerate could be in the metastable superferromagnetic state.

The magnetic weight measurement cannot be employed to investigate the fast dynamics and temperature dependence of magnetic properties, however, slow dynamics induced by magnetic field such as aging, sedimentation, agglomeration, memory effects or phase transition can be studied with good sensitivity by measuring the magnetic weight. Especially detailed examinations of aging and memory will be of a great help to understanding properties of superspin glass state.[46] Also we can inquire into the factors affecting agglomeration of nanoparticles such as coating surfactants, concentration and solvents of ferrofluid, species of nanoparticles, etc. from the magnetic weight measurement. Agglomeration of nanoparticles can be understood better when the energy landscape behind the dynamics is investigated completely.

Acknowledgments. This study was financially supported by research fund of Chungnam National University in 2011.

Supporting Information. The TEM images and the XRD pattern of magnetite nanoparticles used in this work are given in the Supporting Information.

References

1. Lu, A.-H.; Salabas, E. L.; Schüth, F. *Angew. Chem. Int. Ed.* **2007**, *46*, 1222.
2. Yoo, D.; Lee, J.-H.; Shin, T.-H.; Cheon, J. *Acc. Chem. Res.* **2011**, *44*, 863.
3. Lee, J. E.; Lee, N.; Kim, T.; Kim, J.; Hyeon, T. *Acc. Chem. Res.* **2011**, *44*, 893.
4. Gatteschi, D.; Fittipaldi, M.; Sangregorio, C.; Sorace, L. *Angew. Chem. Int. Ed.* **2012**, *51*, 4792.
5. Colombo, M.; Carregal-Romero, S.; Casula, M. F.; Gutierrez, L.; Morales, M. P.; Bohm, I. B.; Heverhagen, J. T.; Prosperi, D.; Parak, W. J. *Chem. Soc. Rev.* **2012**, *41*, 4306.
6. Reddy, L. H.; Arias, J. L.; Nicolas, J.; Couvreur, P. *Chem. Rev.* **2012**, *112*, 5818.
7. Barbeta, V. B.; Jardim, R. F.; Kiyohara, P. K.; Effenberger, F. B.; Rossi, L. M. *J. Appl. Phys.* **2010**, *107*, 073913.
8. Sarkar, D.; Mandal, M. *J. Phys. Chem. C* **2012**, *116*, 3227.
9. Chovnik, O.; Balgley, R.; Goldman, J. R.; Klajn, R. *J. Am. Chem. Soc.* **2012**, *134*, 19564.
10. Rovers, S. A.; Hoogenboom, R.; Kemmere, M. F.; Keurentjes, J. T. F. *J. Phys. Chem. C* **2008**, *112*, 15643.
11. Bedanta, S.; Kleemann, W. *J. Phys. D: Appl. Phys.* **2009**, *42*, 013001.
12. Castillo, V. L. C.-D. del; Rinaldi, C. *IEEE Trans. Magn.* **2010**, *46*, 852.
13. Morales, M. B.; Phan, M. H.; Pal, S.; Frey, N. A.; Srikanth, H. *J. Appl. Phys.* **2009**, *105*, 07B511.
14. Fortin, J.-P.; Wilhelm, C.; Servais, J. Menager, C.; Bacri, J.-C.; Gazeau, F. *J. Am. Chem. Soc.* **2007**, *129*, 2628.
15. Costo, R.; Bello, V.; Robic, C.; Port, M.; Marco, J. F.; Morales, M. P.; Veintemillas-Verdaguer, S. *Langmuir* **2012**, *28*, 178.
16. Jonssona, P. E.; Garcıa-Palaciosb, J. L.; Hansenc, M. F.; Nordblad, P. *J. Mol. Liq.* **2004**, *114*, 131.
17. Poddar, P.; Telem-Shafir, T.; Fried, T.; Markovich, G. *Phys. Rev. B* **2002**, *66*, 060403.
18. Lee, K. R.; Kim, S.; Kang, D. H.; Lee, J. I.; Lee, Y. J.; Kim, W. S.; Cho, D.-H.; Lim, H. B.; Kim, J.; Hur, N. H. *Chem. Mater.* **2008**, *20*, 6738.
19. Vejpravova, J. P.; Tyrpekl, V.; Danis, S.; Niznansky, D.; Sechovsky, V. *J. Magn. Magn. Mater.* **2010**, *322*, 1872.
20. Telem-Shafir, T.; Markovich, G. *J. Chem. Phys.* **2005**, *123*, 204715.
21. Petracica, O.; Chena, X.; Bedanta, S.; Kleemanna, W.; Sahoob, S.; Cardosoc, S.; Freitas, P. P. *J. Magn. Magn. Mater.* **2006**, *300*, 192.
22. Ulrich, M.; Garcıa-Otero, J.; Rivas, J.; Bunde, A. *Phys. Rev. B* **2003**, *67*, 024416.
23. Qi, H.; Chen, Q.; Wang, M.; Wen, M.; Xiong, J. *J. Phys. Chem. C*

2009, *113*, 17301.
24. Jun, B.-H.; Kim, G.; Baek, J.; Kang, H.; Kim, T.; Hyeon, T.; Jeong, D. H.; Lee, Y.-S. *Phys. Chem. Chem. Phys.* **2011**, *13*, 7298.
25. Mohammadi, Z.; Cole, A.; Berkland, C. J. *J. Phys. Chem. C* **2009**, *113*, 7652.
26. Bian, P.; McCarthy, T. J. *Langmuir* **2010**, *26*, 6145.
27. Howes, P.; Green, M.; Bowers, A.; Parker, D.; Varma, G.; Kallumadil, M.; Hughes, M.; Warley, A.; Brain, A.; Botnar, R. *J. Am. Chem. Soc.* **2010**, *132*, 9833.
28. Yavuz, C. T.; Mayo, J. T.; Yu, W. W.; Prakash, A.; Falkner, J. C.; Yean, S.; Cong, L.; Shipley, H. J.; Kan, A.; Tomson, M.; Natelson, D.; Colvin, V. L. *Science* **2006**, *314*, 964.
29. Kang, Y.; Risbud, S.; Rabolt, J. F.; Stroeve, P. *Chem. Mater.* **1996**, *8*, 2209.
30. Berger, P.; Adelman, N. B.; Beckman, K. J.; Campbell, D. J.; Ellis, A. B.; Lisensky, G. C. *J. Chem. Edu.* **1999**, *76*, 943.
31. Sun, S.; Zeng, H. *J. Am. Chem. Soc.* **2002**, *124*, 8204.
32. Lee, Y.; Lee, J.; Bae, C. J.; Park, J.-G.; Noh, H.-J.; Park, J.-H.; Hyeon, T. *Adv. Funct. Mater.* **2005**, *15*, 503.
33. Hagermann, A.; Schnepp, E. *Rev. Sci. Inst.* **2002**, *73*, 2655.
34. Dormann, J. L.; Fiorani, E.; Tronc, E. *Adv. Chem. Phys*. **1997**, *98*, 283.
35. Wiekhorst, F.; Shevchenko, E.; Weller, H.; Kotzler, J. *Phys. Rev. B* **2003**, *67*, 224416.
36. Guardia, P.; Batlle-Brugal, B.; Roca, A. G.; Iglesias, O.; Morales, M. P.; Serna, C. J.; Labarta, A.; Batlle, X. *J. Magn. Magn. Mater.* **2007**, *316*, e756.
37. Masatsugu, S.; Fullem, S. I.; Suzuki, I. S. *Phys. Rev. B* **2009**, *79*, 024418.
38. Roca, A. G.; Morales, M. P.; O'Grady, K.; Serna, C. J. *Nanotech.* **2006**, *17*, 2783.
39. Suzuki, M. *Prog. Theor. Phys*. **1977**, *58*, 1151.
40. Sahoo, S.; Petracic, O.; Binek, Ch.; Kleemann, W.; Sousa, J. B.; Cardoso, S.; Fretas, P. P. *Phys. Rev. B* **2002**, *65*, 134406.
41. Lindsey, C. P.; Patterson, G. D. *J. Chem. Phys*. **1980**, *73*, 3348.
42. Bendler, J. T.; Shlesinger, M. F. *Macromolecules* **1985**, *18*, 591.
43. Klafter, J.; Shlesinger, M. F. *Proc. Natl. Acad. Sci.* **1986**, *83*, 848.
44. Potuzak, M.; Welch, R. C.; Mauro, J. C. *J. Chem. Phys.* **2011**, *135*, 214502.
45. Cuevas, G. D. L.; Faraudo, J.; Camacho, J. *J. Phys. Chem. C* **2008**, *112*, 945.
46. Sahoo, S.; Petracic, O.; Kleemann, W. *Phys. Rev. B* **2003**, *67*, 214422.